ECE 593 Automotive Radar Signal Processing
Term Project

The University of Alabama
Prof. Shunqiao Sun
Fall 2020

1 Introduction

Millimeter-wave technology has found great applicability in automotive radar. The typical frequency band of millimeter-wave automotive radar is 76-81 GHz. The high frequencies allow for small enough antennas that can fit behind the bumper of the vehicle. Also, the wide available bandwidth enables high target range resolution [1]. State-of-the-art automotive radar transmits FMCW at millimeter-wave frequencies, which allows for high resolution target range and velocity estimation at much lower cost than Light Detection and Ranging (LiDAR) technology. Automotive radar for autonomous driving needs to have high angle discrimination capability. Employing a large antenna array would improve angular resolution, however, the resulting large package size would make integration on the vehicle difficult. While for conventional phased-array radar a small package size implies low angular resolution, for MIMO radar [2], package size is not a limiting factor. This is because MIMO radar can synthesize virtual arrays with large aperture using only a small number of transmit and receive antennas [3].

Automotive MIMO radar uses FMCW waveforms along with some mechanism that guarantees waveform orthogonality. This term project will study the radar target detector, waveform orthogonality strategies for automotive radar using FMCW waveforms, virtual array synthesis and angle estimation.

2 State-of-the-art FMCW Radar

An FMCW waveform, also referred to as *chirp*, is a complex sinusoid whose frequency increases linearly with time $t \in [0, T]$, i.e., $f_T(t) = f_c + \frac{B}{T}t$, where B is the signal bandwidth and f_c is the carrier frequency. FMCW radar transmit chirps in a periodic fashion, with a period referred to as pulse repetition interval (PRI). The frequency of an FMCW signal over multiple periods, with PRI equal to T, is shown in Fig. 1. The target echo at the radar receiver contains a delayed and attenuated copy of the transmitted chirp. For a target at range R, moving with radial speed of v, the delay equals $\tau = \frac{2(R+vt)}{c}$, where time t spans multiple periods and c is the speed of light. The received signal is mixed with the transmitted chirp, which results in a complex sinusoid, known as the *beat signal*. The beat signal frequency equals $f_b = f_R + f_D$, where $f_R = \frac{2RB}{Tc}$ is the range frequency and $f_D = \frac{2v}{c}f_c$ is the Doppler frequency. The process of obtaining the beat signal is implemented in the radio-frequency (RF) domain by a mixer followed by a band pass filter (BPF) with maximum cut off frequency $f_b^{\max}$; the latter filter is used to remove signals with frequencies outside the band of interest, which also places a limit to the maximum detectable range. We sample the beat signal and put the samples of each chirp in the columns of a matrix, then the row indices of that matrix correspond to fast time and the column indices to slow time (see Fig. 1). By applying FFTs on the sampled beat signal along fast time, one can identify f_R, based on which the target's range can be obtained as $R = cf_RT/(2B)$. To obtain the target's Doppler frequency, a second FFT operation is subsequently carried out along the slow time (the range frequency f_R is the same across slow time). The application of these two FFTs is equivalent to a two-dimensional (2-D) FFT of the beat signal in fast and slow time, and the result is called *range-Doppler spectrum*. Range and Doppler detection can be performed using conventional thresholding based methods applied to 2-D range-Doppler spectrum, such as the constant false alarm rate (CFAR) detector [4], or the recently proposed deep neural network based detector [5]. Via the 2-D FFT, the targets can be separated in the range and Doppler domain. Since the number of targets within the same range-Doppler bin is small, angle finding can be carried out using sparse sensing techniques, such as compressive sensing.

3 Waveform Orthogonality Strategies

Virtual array synthesis in automotive FMCW radar using MIMO radar technology relies on the separability of the transmit signals of the different antennas. The separation is easier when the transmit signals of different antennas are orthogonal. In the following, we review techniques to achieve waveform orthogonality while transmitting FMCW, such as time division multiplexing (TDM), Doppler division multiplexing (DDM) and frequency division multiplexing (FDM).

In one look, a total of N chirps (i.e., pulses) are transmitted sequentially, with pulse repetition interval T_{PRI}. All transmit antennas transmit simultaneously the same FMCW waveform, after multiplying it with a phase code that is different for each antenna, and changes between pulses, i.e., $x_m(n) = e^{j2\pi\alpha_m(n)}, m = 1, \cdots, M_t, n = 1, \cdots, N$ [6]. To separate the h-th transmit signal at the l-th receiver, after range FFT, a slow time Doppler demodulation

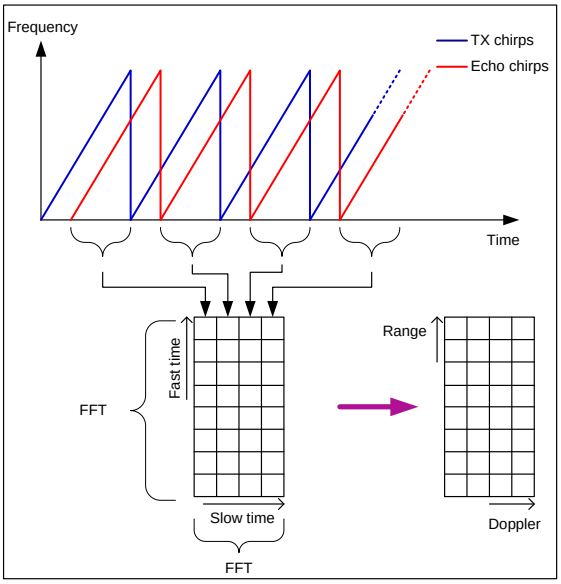

Figure 1: FMCW radar chirps. The range and Doppler estimation is performed using a 2-D FFT.

is applied to all range bins corresponding to the same chirp. The Doppler demodulated outputs of N chirps are assembled into a vector $\mathbf{s}_l^h$. Then, the Doppler FFT is applied on the vector $\mathbf{s}_l^h$. To separate the transmit signals in the Doppler domain, phase codes can be designed such that the Doppler FFT of the interference can be distributed into the entire Doppler spectrum as pseudo noise. It is desired to minimize the peak interference residual (PIR) in the Doppler spectrum [7] calculated using the discrete-time Fourier transform (DTFT) for $m = 1, \cdots, M_t$, i.e.,

$$\text{PIR} = \max_{f, m \neq h} \left| \sum_{n=1}^{N} e^{j2\pi(\alpha_m(n) - \alpha_h(n))} e^{j2\pi f n} \right|, \tag{1}$$

where $f \in \left[-\frac{1}{2} f_{\text{PRF}}, \frac{1}{2} f_{\text{PRF}}\right]$. Following equation (1), the cross-correlation of the spectra of two codes needs to be flat [7], since the Fourier transform of multiplication of two codes in the time domain is equivalent to convolution of spectrum of one code with time reversed and complex conjugate of the other. The maximum auto-correlation value of an unimodular sequence of length N is N. The ideal cross-correlation of two unimodular sequences of length N has magnitude of $\sqrt{N}$. Thus, in the ideal case, according to [7] the maximum power gain of the currently transmitted signal over other signals is $\sqrt{N}$.

Constant amplitude zero auto-correlation codes are good candidates for DDM. The discrete Fourier transform (DFT) of a constant amplitude zero auto-correlation code has also constant amplitude and zero auto correlation[8]. One of such examples is the Chu sequence [9], which is defined as $x_m(n) = e^{\frac{j\pi}{N} m(n+1)n}, m = 1, \ldots M_t, n = 1, \ldots, N$, where N is a prime number. In practice, the Chu sequence of prime length is first generated and then truncated into a length for efficient FFT. For example, we generate Chu codes of prime length 521 and truncate them to length $N = 512$. By calculation with FFT, the peak interference residual defined in (1) is $1.08\sqrt{N}$. Therefore, the waveform attenuation for Chu sequence of length $N = 512$ is about 26.4dB. In Fig. 2 (b), we show the range and Doppler spectrum of a target with range of 75m and velocity of 10m/s. The automotive radar has two transmit antennas and two Chu sequences of length $N = 512$ are applied for slow time DDM. It can be seen that the waveform attenuation is about 26dB.

In practice, binary phase codes are used due to hardware constraint [10]. The binary phase code sequences are obtained via exhaustive search such that the peak interference residual in (1) is low. As the code length increases, the search time will grow exponentially.

4 Virtual Array Synthesis and Angle Estimation

In automotive MIMO radar with M_t transmit and M_r receive antennas, a virtual uniform linear array of $M_t M_r$ elements can be synthesized with inter-element spacing d. The array response can be written as

$$\mathbf{y} = \mathbf{A}(\theta)\mathbf{s} + \mathbf{n}, \tag{2}$$

where $\mathbf{A}(\theta) = [\mathbf{a}(\theta_1), \cdots, \mathbf{a}(\theta_K)]$ is the virtual array steering matrix with

$$\mathbf{a}(\theta_k) = \left[1, e^{j\frac{2\pi}{\lambda} d \sin(\theta_k)}, \cdots, e^{j\frac{2\pi}{\lambda}(M_t M_r - 1) d \sin(\theta_k)}\right]^T. \tag{3}$$

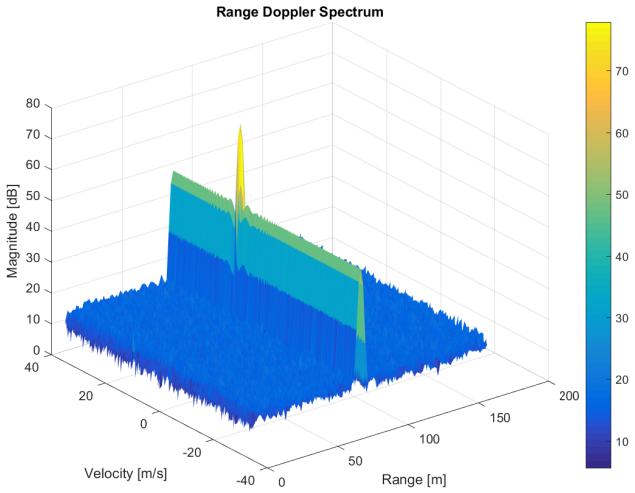

Figure 2: The range and Doppler spectra of a target with range of 75m and velocity of 10m/s. The automotive MIMO radar has two transmit antennas and slow time phase coding using Chu sequence of length $N = 512$ is applied for DDM.

Here, $\mathbf{n}$ is a noise term and $\mathbf{s} = [\beta_1, \cdots, \beta_K]^T$, where β_k denotes the target reflection coefficient for the k-th target. The array response at a particular time instance consisting of data obtained at all the virtual receivers and corresponding to the same range-Doppler bin is defined as the *array snapshot*.

In automotive MIMO radar with virtual uniform linear array (ULA), angle finding can be done with digital beamforming (DBF) [11] by performing FFTs on snapshots taken across the array elements, , i.e., $\mathbf{y}$ in equation (2) (see Fig. 3). DBF can be implemented efficiently in an embedded DSP with a single snapshot. However, DBF is not a high resolution angle finding method. Higher resolution angle finding can be achieved with subspace based methods, such as MUSIC [12] and compressive sensing [13, 14].

5 Objective and Expectation

You can choose either one of following three projects to work on.

Project 1: CFAR Implementation Tasks: 1) Run automotive FMCW radar simulator in Matlab; 2) CA-CFAR on range-Doppler spectrum; 3) OS-CFAR on range-Doppler spectrum.

Project 2: Angle Estimation with Virtual Array Tasks: 1) Run automotive FMCW radar simulator in Matlab; 2) Synthesize virtual array (you can use Chu sequence for orthogonality); 3) Angle estimation with FFT, MUSIC and Compressive Sensing for virtual ULA.

Project 3: DDM Implementation Tasks: 1) Run automotive FMCW radar simulator in Matlab; 2) Implement DDM via Chu sequence; 3) Binary phase coding search for DDM.

Term Paper and Presentation You can form a team with two members to work on the project. Each team should submit a final term paper followed by a presentation (25 minutes) on Dec. 2 (Wednesday) and Dec. 4 (Friday), 10:00AM-10:50AM. The term paper is due at 11:59PM, Saturday, Dec. 12, 2020. Suggested contents in the term paper and presentation are

- Background introduction/literature review
- System modeling and problem formulation
- Introduction of solution algorithms
- Numerical results and analysis in Matlab
- Summary or conclusions
- Matlab scripts (attachment)

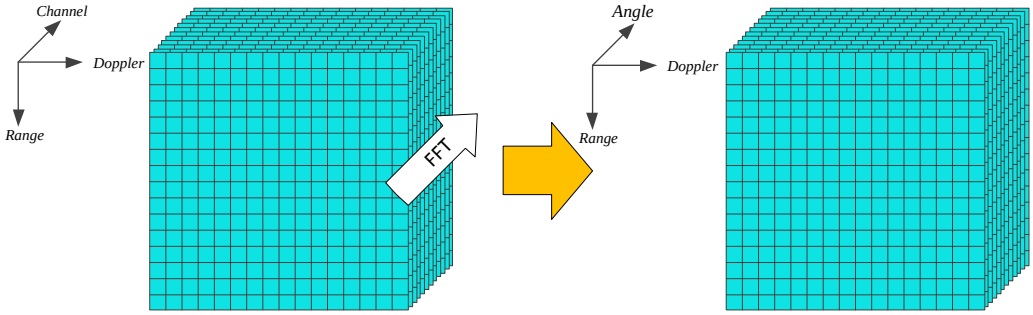

Figure 3: Digital beamforming (DBF).

References

[1] J. Hasch *et. al.*, "Millimeter-wave technology for automotive radar sensors in the 77 GHz frequency band," *IEEE Trans. Microw. Theory Tech.*, vol. 60, no. 3, pp. 845–860, 2012.

[2] J. Li and P. Stoica, "MIMO radar with colocated antennas," *IEEE Signal Process. Mag.*, vol. 24, no. 5, pp. 106–114, 2007.

[3] S. Sun, A. P. Petropulu, and H. V. Poor, "MIMO radar for advanced driver-assistance systems and autonomous driving: Advantages and challenges," *IEEE Signal Process. Mag.*, vol. 37, no. 4, pp. 98–117, 2020.

[4] M. A. Richards, *Fundamentals of Radar Signal Processing, 2nd Ed.* New York, NY: McGraw-Hill, 2014.

[5] D. Brodeski, I. Bilik, and R. Giryes, "Deep radar detector," in *Proc. IEEE Radar Conf.*, Boston, MA, April 2019.

[6] V. F. Mecca, D. Ramakrishnan, and J. L. Krolik, "MIMO radar space-time adaptive processing for multipath clutter mitigation," in *Proc. IEEE Workshop on Sensor Array and Multichannel Processing (SAM)*, Waltham, MA, July 2006.

[7] N. Madsen and S. Cao, "Slow-time waveform design for MIMO GMTI radar using CAZAC sequences," in *Proc. IEEE Radar Conf.*, Oklahoma City, OK, April 2018.

[8] J. Benedetto, I. Konstantinidis, and M. Rangaswamy, "Phase-coded waveforms and their design," *IEEE Signal Process. Mag.*, vol. 26, no. 1, pp. 22–31, 2009.

[9] D. Chu, "Polyphase codes with good periodic correlation properties," *IEEE Trans. Inf. Theory*, vol. 18, no. 4, pp. 531–532, 1972.

[10] R. Feger, H. Haderer, and A. Stelzer, "Optimization of codes and weighting functions for binary phase-coded FMCW MIMO radars," in *Proc. Intl. Conf. Microwaves for Intelligent Mobility (ICMIM)*, San Diego, CA, May 2016.

[11] P. Barton, "Digital beam forming for radar," *IEE Proc. F - Commun., Radar and Signal Processing*, vol. 127, no. 4, 1980.

[12] R. Schmidt, "Multiple emitter location and signal parameter estimation," *IEEE Trans. Antennas Propag.*, vol. 34, no. 3, pp. 276–280, 1986.

[13] Y. Yu, A. P. Petropulu, and H. V. Poor, "MIMO radar using compressive sampling," *IEEE J. Sel. Topics Signal Process.*, vol. 4, no. 1, pp. 146–163, 2010.

[14] Y. Yu, S. Sun, R. N. Madan, and A. P. Petropulu, "Power allocation and waveform design for the compressive sensing based MIMO radar," *IEEE Trans. Aerosp. Electron. Syst.*, vol. 50, no. 2, pp. 898–909, 2014.